J Mol Model (2013) 19:1651–1666
DOI 10.1007/s00894-012-1726-3

ORIGINAL PAPER

Targeted molecular dynamics (TMD) of the full-length KcsA potassium channel: on the role of the cytoplasmic domain in the opening process

Yan Li · Florent Barbault · Michel Delamar · Ruisheng Zhang · Rongjing Hu

Received: 10 August 2012 / Accepted: 5 December 2012 / Published online: 5 January 2013

Abstract Some recent papers clearly indicate that the cytoplasmic domain of KcsA plays a role in pH sensing. We have performed, for the first time, a targeted molecular dynamics (TMD) simulation of the opening of full-length KcsA at pH 4 and pH 7, with a special interest for the cytoplasmic domain. Association energy calculations show a stabilization at pH 7 confirming that the protonation of some amino-acids at pH 4 in this domain plays a role in the opening process. A careful analysis of the pH dependent charges borne by residues in the cytoplasmic domain and their interactions confirms some literature experimental data and permits to give further insight into the role played by some of them in the opening process.

Keywords Cytoplasmic domain · Full-length KcsA · pH sensor · Targeted molecular dynamics (TMD)

Electronic supplementary material The online version of this article (doi:10.1007/s00894-012-1726-3) contains supplementary material, which is available to authorized users.

Y. Li · R. Zhang
Department of Chemistry, Lanzhou University, Lanzhou, Gansu 730000, People's Republic of China

R. Zhang · R. Hu
School of Information Science and Engineering, Lanzhou University, Lanzhou, Gansu 730000, People's Republic of China

Y. Li · F. Barbault · M. Delamar (✉)
Univ Paris Diderot, Sorbonne Paris Cité, ITODYS, UMR CNRS 7086, 15 rue J-A. de Baïf, 75013 Paris, France
e-mail: michel.delamar@univ-paris-diderot.fr

Introduction

Ion channels are transmembrane proteins which allow ions to diffuse across biological membranes through an internal pore located in the channel center [1].

Active channels have gates which can open and close to control the ionic fluxes under some specific stimulus, such as voltage, ligand binding, temperature, pH and mechanical tension [2, 3]. Gating involves two processes: (i) a sensing step and (ii) a structural rearrangement initiated by (i) (see [4] and references therein).

Potassium channels are found in bacteria, yeast, *Paramecia*, plants and animal cells, including electrically excitable tissues as well as unexcitable tissues, such as the liver and cells of the immune system [5]. They are involved in nerve and muscles excitation and in a number of pathological processes [1, 6].

KcsA, a prokaryotic potassium (K^+) channel from *Streptomyces lividans* is activated by intracellular protons [7, 8]. It has been extensively studied [2, 4, 6–29] because of its similarity to eukaryotic channels. KcsA was first described in 1995 [9], and its three-dimensional structure was first characterized by X-ray crystallography at 3.2 Å resolution in 1998 (PDB code 1BL8) [10]. Then a better resolution (2.0 Å) was achieved [11] for the open-inactivated conformation using a monoclonal antigen-binding fragment (Fab) fragment as crystallographic chaperone (PDB code 1K4C).

Uysal et al. [6] have used synthetic Fabs to determine the structure of the full-length KcsA at 3.8 Å resolution in its closed conformation. They also determined the structure of its isolated C-terminal domain at 2.6 Å. Cuello et al. [27] also reported the crystal structure of KcsA, from its closed-conductive to its open-inactivated conformation and studied

C-type inactivation. They identified five conformers with openings from 12 Å to 32 Å.

This channel is a tetramer with a transmembrane (TM) domain (120 residues) and a cytoplasmic domain (*ca*. 40 residues) [6]. The tetramer is formed by four identical subunits, each consisting of three parts [6, 30]:

- a transmembrane (TM) domain containing two transmembrane segments, the outer-helix TM1 and the inner-helix TM2. TM1 is close to the N terminus and is exposed to the membrane bilayer. TM2 is close to the C terminus and contributes to the lining of the pore.
- a re-entrant P loop made by a P-helix (P) and a selectivity filter (SF) containing the characteristic motif of all potassium channels, a *TVGYG* sequence. Cuello et al. [27] studied the conformation and ion occupancy of the selectivity filter during channel opening.
- a cytoplasmic domain rich in charged or polar amino acid residues. The cytoplasmic domain of most channels plays an important role in sensing, gating, permeation, and structural stability ([21, 30] and references therein). Uysal et al. [6] showed that the cytoplasmic domain of KcsA "remains essentially intact" during opening of the channel.

The gating mechanism of the KcsA channel has been extensively studied using a number of methods: site-directed spin-labelling and EPR [14, 15], X-ray crystallography [11], comparison of open and closed structures (respectively MthK from *Methanobacterium thermoautotrophicum* and KcsA) [16].

It was then proposed [13, 31, 32] that the cytoplasmic part and more precisely the C-terminal domain was the locus of the pH sensor.

Takeuchi et al. [18] using NMR evidenced the protonation of His25 and considered this residue to be the pH-sensor. Thompson et al. [17] using mutations proposed a pH sensing and opening mechanism in which the interactions which keep the channel in closed form are suppressed by the protonation of several residues (Arg122 and Glu120 on the TM2 helices and to some extent His25) provoking TM2 conformational changes.

Cuello et al. [4] confirmed these findings using mutations, spin-labeling and EPR and electrostatic calculations: electrostatic attractive/repulsive balance between a cluster of charged groups (especially Arg117, Glu118, Glu120 at the bottom of TM2 and His25 at the end of TM1) contribute to channel opening.

Hirano et al. [20] also reported that the four C-terminus of TM2 form a network that stabilizes the closed state in neutral condition while the network is disrupted when the intracellular pH is acidic. Then the TM2 helices bend, causing channel opening.

Uysal et al. [21] confirmed that the movement of gating parts of TM2 helices was transmitted to the C-terminus as a straightforward expansion, which led to an upward movement of the cytoplasmic domain and insertion of some parts into the membrane.

Hirano et al. [33] have clearly shown that charged amino acids in the cytoplasmic domain play an important role in pH dependent gating by replacing residues that are negatively charged at pH 7 with neutral ones: the opening was then independent of pH. The Glu146 and Asp149 residues were thus shown to play a role in the opening process. These results demonstrated that the cytoplasmic domain acts as a pH sensor, together with the transmembrane region [4, 34].

Of course, modeling and simulation techniques have been used for more than 10 years to investigate the opening dynamics and K^+ permeation in the KcsA and related K^+ channels (see [26] and references therein). Holyoake et al. [26] used homology modeling to propose models for the TM domain in the open state of KcsA and performed MD simulations with a membrane mimetic octane slab. They confirmed that M2 bending leads to a stable open state and observed K^+ ions trajectories exiting toward the intracellular medium.

Compoint et al. [23, 24] used targeted molecular dynamics (TMD) with a membrane mimetic octane slab to simulate the pore opening of the KcsA channel. They invoked a "ziplike" opening mechanism and evidenced the role of the terminal residues on the M2 helices. A possible diffusion of K^+ ions toward the extracellular side was also observed. TMD and SMD (steered molecular dynamics) were used by Zhong et al. [22, 25] who showed that during the opening water molecules can penetrate the cavity and facilitate the process. Cuello et al. [35] produced a detailed study of the interactions between some residues during gating and invoked a network of interactions resulting in the propagation of a mechanical deformation during the opening process. Interaction energies obtained from MD showed the important role played by Phe 103 and surrounding residues. An approach aimed at determining the energetics of the gating process was recently proposed by Kharkyanen et al. [36].

Numerous structural biology studies have been performed and provide precious and meaningful information on the KcsA structure, mainly for the truncated system. However, the KcsA full-length structures have only been studied by X-ray crystallography [6, 21] and thus the ionization state of the amino-acids is missing. Molecular modeling simulations, based on the experimental structures like the TMD method, can help to decipher the role of the protonation on the cytoplasmic domain of KcsA to the opening process.

In this paper we perform, for the first time to our knowledge, targeted molecular dynamics (TMD) on the complete system. The aim of this work is to study the influence of the

cytoplasmic domain on the gating mechanism of KcsA at two specific pH conditions, not the opening process nor the ions diffusion which have been previously thoroughly examined. After establishing the conditions for TMD on such a system, we especially compare our results with the above-mentioned experimental ones obtained with mutant systems about the role of some residues in the cytoplasmic domain in the opening process. We also compare our results, obtained with a full length KcsA, with some experimental ones obtained with truncated systems.

Methods

KcsA is a membrane protein. Therefore, it may be envisioned to simulate the whole system, with the channel inserted in a membrane and water molecules around. In this case periodic conditions must be used to ensure system integrity. However it is necessary to hypothesize the fact that a large motion of the cytoplasmic domain may occur. For example, the cytoplasmic α-helices bundle might open and extend. In such a case, a collision between the protein and its own periodic image will happen [37] if the width of the periodic box is not at least equal to the length of the cytoplasmic domain (around 80 Å). Considering this requirement, called minimum image convention, such a system would consist of *ca*. 500,000 atoms (among which *ca*. 380,000 would be atoms of water molecules).

We used targeted molecular dynamics simulations, using the opened and close states of the channel, as a driving force to study the conformational changes of the cytoplasmic domain at two different pH values. Therefore, we made these simulations with implicit solvent to save computational time and then focused on the simulation of the cytoplasmic domain. This assumption limited our calculations to only 8308 atoms and avoided long computation time devoted to the equilibration of membrane and water. Moreover, both for coherence of this approach and in order to focus this work on the behavior of the cytoplasmic domain, constraints were applied to the transmembrane domain so that our results in what follows concern mainly the cytoplasmic domain.

Description of simulation systems

Our initial structure was from a crystallized experimental full-length closed structure (PDB code 3EFF) of the KcsA channel at 3.8 Å resolution [6]. The targeted structure was the fully open state (Cα-Cα distances at Thr 112 are 32 Å) of KcsA channel from a crystallized experimental structure (PDB code 3F5W) at 3.2 Å resolution [27].

The closed structure of the KcsA channel at 2.0 Å resolution (PDB code 1K4C) was determined [11], together with seven sites for the K^+ ions. Two of these are located at the extracellular side of the pore (S_0 and S_{ext}), four are located inside the selectivity filter (S_1, S_2, S_3, S_4) and one is in the central cavity (S_{cav}). As in the work of Compoint et al. [28] only six sites were considered in our simulations since the S_{ext} site only appears at high K^+ concentration. The precise structural definition of these sites can be found in the paper of Cuello et al. [27].

Zhou et al. [11] and Morais-Cabral et al. [29], based on crystallographic distances between K^+ ions, argued that the four selectivity filter sites are not all occupied simultaneously, rather, they are often separated by an intervening water molecule. Thus, as other authors [23, 27, 28], we studied the K …K…K sequence (three K^+ ions located at the S_1, S_3 and S_{cav} sites) and the KWKWK…K sequence (four K^+ ions located at the S_0, S_2, S_4 and S_{cav} sites and two water molecules at the S_1, and S_3 sites.

The full length structure contains numerous atoms. Therefore, to save calculation time, we defined the best set of parameters with systems including only the TM domains.

Thus, a total of six systems were prepared (Table 1):

- the first one (CH0) included only the channel domain without any K^+ ions and water molecules
- two systems (CH1, CH2) included only the channel domain: CH1 with the K…K…K sequence and CH2 with the KWKWK…K sequence.
- two other systems (F1, F2) included the full-length structure with the KWKWK…K sequence with TM and cytoplasmic domains, at different pH conditions (4 and 7 respectively). For F1, protonation has been taken into account in the cytoplasmic region only.

The location of potassium ions in the KcsA cavities has been often debated [11, 23, 27–29]. Therefore, we tested the K…K…K sequence for CH1 and the KWKWK..K sequence for CH2. We did not intend to observe ionic behavior such as permeation and/or selectivity since these events occur only for the open conformation of the channel. We employed the KWKWK..K sequence for systems F1 and F2 since it was reported that this one more strongly stabilizes the KcsA channel [28]. Systems F3 and F4 were prepared from Cuello et al. [4]:

- the F3 system was analogous to the F1 system, except that at this pH value of 4 we wished to study the effect of protonation of two more residues (Glu118 and Glu120) located at the limit between the TM and cytoplasmic domains.
- the F4 system was analogous to F3 but we introduced the His25 protonated residue since as mentioned above, several authors identified His25 as being part of the pH-sensor that controls the pH-dependent gating of KcsA.

Table 1 Amino-acid sequences of the simulation systems studied in this work. Systems CH0, CH1 and CH2 are limited to the channel region: TM domains (TM1 + TM2) are enclosed in red squares. The protonation state is indicated by colors for the cytoplasmic domain only. Blue = positively charged amino-acids. Orange = negatively charged residues. Green = residues which are usually ionic but are neutral at the considered pH

Channel CH0 (no ion)

```
   30                                                                                                  112
(A)GAATVLLVIVLLAGSYLAVLAERGAPGAQLITYPRALWWSVETATTVGYGDLYPVTLWGRLVAVVVMVAGITSFGLVTAALAT
(B)GAATVLLVIVLLAGSYLAVLAERGAPGAQLITYPRALWWSVETATTVGYGDLYPVTLWGRLVAVVVMVAGITSFGLVTAALAT
(C)GAATVLLVIVLLAGSYLAVLAERGAPGAQLITYPRALWWSVETATTVGYGDLYPVTLWGRLVAVVVMVAGITSFGLVTAALAT
(D)GAATVLLVIVLLAGSYLAVLAERGAPGAQLITYPRALWWSVETATTVGYGDLYPVTLWGRLVAVVVMVAGITSFGLVTAALAT
              TM1                                                                    TM2
```

Channel CH1 (K…K…K)

```
   30                                                                                                  112
(A)GAATVLLVIVLLAGSYLAVLAERGAPGAQLITYPRALWWSVETATTVGYGDLYPVTLWGRLVAVVVMVAGITSFGLVTAALAT
(B)GAATVLLVIVLLAGSYLAVLAERGAPGAQLITYPRALWWSVETATTVGYGDLYPVTLWGRLVAVVVMVAGITSFGLVTAALAT
(C)GAATVLLVIVLLAGSYLAVLAERGAPGAQLITYPRALWWSVETATTVGYGDLYPVTLWGRLVAVVVMVAGITSFGLVTAALAT
(D)GAATVLLVIVLLAGSYLAVLAERGAPGAQLITYPRALWWSVETATTVGYGDLYPVTLWGRLVAVVVMVAGITSFGLVTAALAT
              TM1                                                                    TM2
```

Channel CH2 (KWKWK…K)

```
   30                                                                                                  112
(A)GAATVLLVIVLLAGSYLAVLAERGAPGAQLITYPRALWWSVETATTVGYGDLYPVTLWGRLVAVVVMVAGITSFGLVTAALAT
(B)GAATVLLVIVLLAGSYLAVLAERGAPGAQLITYPRALWWSVETATTVGYGDLYPVTLWGRLVAVVVMVAGITSFGLVTAALAT
(C)GAATVLLVIVLLAGSYLAVLAERGAPGAQLITYPRALWWSVETATTVGYGDLYPVTLWGRLVAVVVMVAGITSFGLVTAALAT
(D)GAATVLLVIVLLAGSYLAVLAERGAPGAQLITYPRALWWSVETATTVGYGDLYPVTLWGRLVAVVVMVAGITSFGLVTAALAT
              TM1                                                                    TM2
```

System F1 (KWKWK…K): pH = 4

```
          30         113
(A)SALHWRAA- channel -WFVGREQERRGHFVRHSEKAAEEAYTRTTRALHERFDRLERMLDDNRR
(B)SALHWRAA- channel -WFVGREQERRGHFVRHSEKAAEEAYTRTTRALHERFDRLERMLDDNRR
(C)SALHWRAA- channel -WFVGREQERRGHFVRHSEKAAEEAYTRTTRALHERFDRLERMLDDNRR
(D)SALHWRAA- channel -WFVGREQERRGHFVRHSEKAAEEAYTRTTRALHERFDRLERMLDDNRR
```

System F2 (KWKWK…K): pH = 7

```
          30         113
(A)SALHWRAA- channel -WFVGREQERRGHFVRHSEKAAEEAYTRTTRALHERFDRLERMLDDNRR
(B)SALHWRAA- channel -WFVGREQERRGHFVRHSEKAAEEAYTRTTRALHERFDRLERMLDDNRR
(C)SALHWRAA- channel -WFVGREQERRGHFVRHSEKAAEEAYTRTTRALHERFDRLERMLDDNRR
(D)SALHWRAA- channel -WFVGREQERRGHFVRHSEKAAEEAYTRTTRALHERFDRLERMLDDNRR
```

System F3 (KWKWK…K): pH = 4

```
          30         113
(A)SALHWRAA- channel -WFVGREQERRGHFVRHSEKAAEEAYTRTTRALHERFDRLERMLDDNRR
(B)SALHWRAA- channel -WFVGREQERRGHFVRHSEKAAEEAYTRTTRALHERFDRLERMLDDNRR
(C)SALHWRAA- channel -WFVGREQERRGHFVRHSEKAAEEAYTRTTRALHERFDRLERMLDDNRR
(D)SALHWRAA- channel -WFVGREQERRGHFVRHSEKAAEEAYTRTTRALHERFDRLERMLDDNRR
```

System F4 (KWKWK…K): pH = 4

```
     25   30         113
(A)SALHWRAA- channel -WFVGREQERRGHFVRHSEKAAEEAYTRTTRALHERFDRLERMLDDNRR
(B)SALHWRAA- channel -WFVGREQERRGHFVRHSEKAAEEAYTRTTRALHERFDRLERMLDDNRR
(C)SALHWRAA- channel -WFVGREQERRGHFVRHSEKAAEEAYTRTTRALHERFDRLERMLDDNRR
(D)SALHWRAA- channel -WFVGREQERRGHFVRHSEKAAEEAYTRTTRALHERFDRLERMLDDNRR
```

Determination of pKa values

Since KcsA is a pH dependent channel we constructed two kinds of simulation systems at low and neutral pH to investigate the location of the "pH sensor" and the role of the cytoplasmic domains in channel gating. Of importance in this study was the protonation state of ionizable residues in the cytoplasmic domains of KcsA at low pH and neutral pH. To determine the pKa values of these titratable residues in the cytoplasmic domains of KcsA, the structure file of the

cytoplasmic domains (residues 113–160) was submitted to Virginia Tech's H++ server (http://biophysics.cs.vt.edu/H++), a Web-based system that computes pKa values of ionizable groups in proteins based on the Poisson-Boltzmann (PB) or generalized Born (GB) models [38]. The pKa calculations were performed using default values: internal dielectric constant of 4, external dielectric constant of 80, ionic strength of 0.15 M, and pH values of 4 and 7. These calculations yield at each pH the protonation state of each amino acid (Table 1).

Targeted MD

Targeted molecular dynamics (TMD) [39] has been proven of great interest in relating protein dynamics and function [40]. It aims at obtaining a target structure from a starting structure by avoiding accidental conformational changes during molecular dynamics simulations through the application of a time-dependent constraint:

$$V = \frac{k}{2N}[RMSD(t) - RMSD_0(t)]^2, \quad (1)$$

where k is the force constant, RMSD(t) is the RMSD of the structure at time t, relative to the target structure, $RMSD_0(t)$ is the prescribed RMSD of the target at time t and N is the number of concerned atoms.

In this work, we brought the closed state to open state by TMD. The Cα atoms of the two transmembrane helices (TM) of KcsA (residues 33–50 and 86–114)[1] were restrained to the corresponding positions of the target structure (PDB code 3F5W).

All the MD simulations were performed with the AMBER11 [41] software using the ffSB99 force field. The generalized Born/surface area model (GB/SA) implicit model was used instead of explicit water during MD simulation.

Energy minimization of all the initial structures (closed and open states) was carried out using the steepest descent method in AMBER11 for 500 steps and the nonbonded cut-off was 99 Å.

A series of preliminary simulations was carried out to determine an appropriate value of the TMD force constant. For non-bonding interactions no cut-off was applied. The SHAKE algorithm [42] was used to fix the length of all bonds involving hydrogen and the time step was 0.002 ps. We used Langevin dynamics at 300 K with a collision frequency of 2 ps^{-1}. The temperature coupling method was used to keep the temperature constant at 300 K and Langevin dynamics was used. The total simulation time was 10 ns.

[1] Except for the full systems simulations where residues 113 and 114 were not restrained since they are located at the border between TM and cytoplasmic domains.

Then the full system was investigated at pH 7 and pH 4 with different protonated residues.

Free energy calculations

MM-GBSA analyses were employed to evaluate the association energy between the four units of the KcsA channel. To distinguish the contributions of the cytoplasmic and those of the trans-membrane domains, we modified the snapshots extracted for the whole systems: for all units, the residues involved in the transmembrane domain (residues 22 to 111) were removed and residue 112 was mutated as an acetyl group in order to avoid the formation of a protonated N-terminal residue. Then we calculated the binding free energies between these four units only for the cytoplasmic coordinates extracted from the TMD of the whole systems. The energetic contribution of the membrane domain is the difference between the total binding free energy and the contribution of the cytoplasmic part.

The free energy of binding, ΔG, for each species can be calculated by using the following scheme:

$$\begin{aligned}
\Delta G &= \Delta E_{gas} + \Delta G_{sol} - T\Delta S_{gas} \\
\Delta E_{gas} &= \Delta E_{int} + \Delta E_{ele} + \Delta E_{VdW} \\
\Delta E_{int} &= \Delta E_{bond} + \Delta E_{angle} + \Delta E_{torsion} \\
\Delta S_{gas} &= \Delta S_{translation} + \Delta S_{rotation} + \Delta S_{vibration} \\
\Delta G_{sol} &= \Delta G_{GB} + \Delta G_{nonpolar} \\
\Delta G_{nonpolar} &= \gamma SASA
\end{aligned}$$

where ΔE_{gas} is the gas-phase energy; T and ΔS are the temperature and the total solute entropy. For gas phase, the entropic contributions were divided into translational, rotational, and vibrational motions. The first two terms were obtained from classical statistical mechanics, whereas the contribution from vibrational motion was estimated from a normal mode analysis according to the method developed by Kottalam and Case [43].

ΔE_{int} is the internal energy; ΔE_{bond}, ΔE_{angle}, and $\Delta E_{torsion}$ are the bond, angle, and torsion energies, respectively; ΔE_{ele} and ΔE_{VdW} are the Coulomb and van der Waals energies. ΔG_{sol} is the solvation free energy, decomposed into polar and nonpolar contributions. ΔG_{GB} is the polar solvation contribution calculated by solving GB equations. $\Delta G_{nonpolar}$ is the nonpolar solvation contribution. SASA is the solvent accessible surface area. γ is the surface tension.

ΔE_{gas} was calculated using the AMBER ff99SB force field. Dielectric constants for solute and solvent were set to 1 and 80, respectively. $\Delta G_{nonpolar}$ was estimated from SASA determined by LCPO method using a water probe radius of 1.4 Å. The surface tension constant was set to 0.0072 kcal mol^{-1} $Å^{-2}$ [44]. Snapshots, equally spaced at 100 ps intervals, were extracted from the MD production runs, giving 100 snapshots for 10 ns.

TMD simulations

Multiple targeted molecular dynamics (MTMD): setting up simulation parameters

The KcsA channel has been extensively described in the past, so that numerous structures are available. On a first approach, we took advantage of the partially opened structures of KcsA and thus we performed multiple target molecular dynamics (MTMD) simulations. We used the closed state of KcsA channel at 3.8 Å resolution as initial structure (PDB code 3EFF) [6] and the targeted structures were the open state and four partially open states (TM domains only). These partially open states and a fully open state (Cα-Cα distances at Thr112 ranging from 14.5 to 32 Å) state were experimental structures designated by open 32, open 23, open 17, open 16 and open 14 (respective PDB codes 3F5W, 3F7V, 3F7Y, 3FB6, 3FB5) of KcsA channel at 3.2 Å resolution [27]. However, in the six experimental structures, the total number of residues was different. In order to keep the same whole sequence in the simulations, we retained a common structure with residues 30–114 and removed the other residues. In these calculations, a restraint was added to bring the closed state to open 14, then from open 14 to open 16, open 16 to open 17, open 17 to open 23, and open 23 to open 32. We choose the Cα atoms of the two transmembrane helices (TM) of KcsA (residues 33–50 and 86–114) to be restrained to the corresponding positions of the reference structure.

We determined the RMSD values between the different structures and those relative to the closed one from literature values. As Table 2 shows, there are little structural changes from open 14 to open 17, but the structure undergoes significant changes from open 17 to open 23 and a slight change from open 23 to open 32. We performed productions of 10 ns with three different force constant values: 50, 10 and 5 kcal mol^{-1} $Å^{-2}$ and we monitored the RMSD curves of the transmembrane domain (TM) along the TMD trajectories. Figure 1 indicates that no meaningful structural variation is observed between these three values. We also calculated the maximum amount of restraint energy provided during the simulations for the three force constants which

Table 2 RMSD values (Cα of TM) between different structures (from literature results [6, 27])

System	RMSD Å	System	RMSD Å
closed↔open14	1.71604	closed↔open14	1.71604
open14↔open16	0.25303	closed↔open16	1.72935
open16↔open17	0.26589	closed↔open17	1.74869
open17↔open23	2.20162	closed↔open23	3.62312
open23↔open32	1.79433	closed↔open32	3.94623

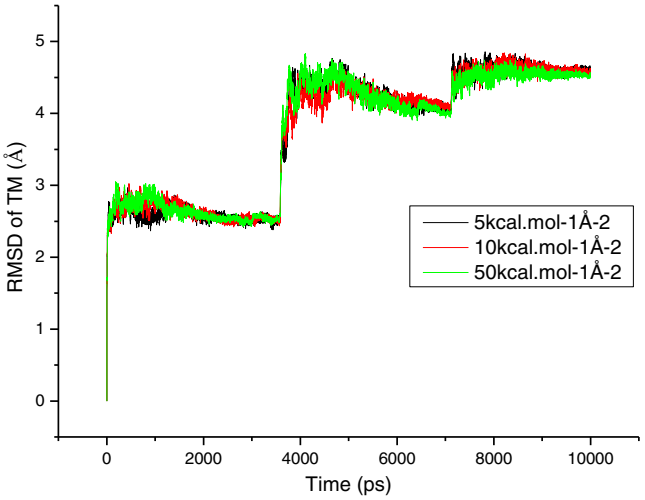

Fig. 1 RMSD of the TM domain (CH2 system) with different force constants along the overall production of the dynamics (10 ns)

were 123, 87 and 74 kcal mol^{-1} when the force constant was 50, 10 and 5 kcal mol^{-1} $Å^{-2}$ respectively. Whereas Compoint et al. [23, 24] used values up to 12 kcal mol^{-1} $Å^2$, these preliminary results showed that a force constant of 5 kcal mol^{-1} $Å^2$ is appropriate. Lower values would probably be insufficient for the whole system to evolve from the closed to the open state.

These results also confirm that the atom selection (Cα-Cα) required to perform the transition between close to open states of the channel was correct and the simulation time (10 ns) was long enough to observe the transition. It may be observed that the force constant we used is quite small and the restraint energy is of the order of 1.5 % compared to the global energy. It is also interesting to point out that we reproduced the evolution from the closed form to the open form without the simulation of the membrane.

TMD without intermediate structures

Classical TMD was then performed with the same parameters except that we imposed no intermediate structures between the initial and final conformations. By monitoring the RMSD of full length systems F1 and F2 relative to the above mentioned intermediate structures we tried to check that they were indeed encountered on the trajectory. The RMSD differences between the closed conformation and the first intermediate conformations (up to open 17) are rather small and similar (Table 2) but it was possible, during the TMD simulation, to observe a RMSD minimum at 6.25 ns with the intermediate structure open 23 (as the reference structure) showing that this conformation is indeed observed during TMD (Fig. 2). A continuous RMSD decrease toward the open 32 conformation was also obtained, as expected.

In the following work we did not use the intermediate structures since this was revealed not necessary and this is

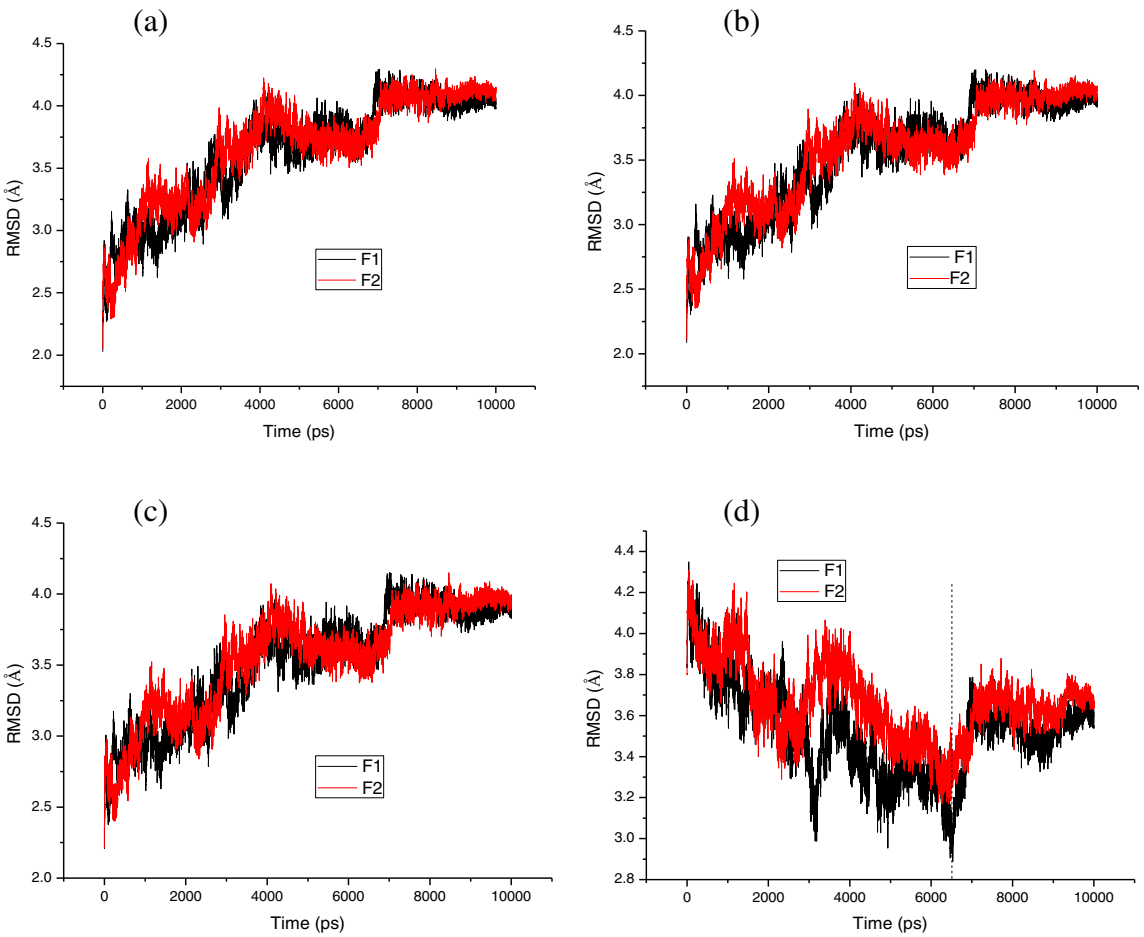

Fig. 2 Cα RMSD of TM2 for systems F1 (pH 4) and F2 (pH 7) along the overall production of the dynamics (10 ns). The reference structures are open 14 (**a**), open 16 (**b**), open 17 (962), open 23 (**d**)

the first time, to our knowledge, that TMD was performed on the full system from closed to open form.

TMD of the four full length simulation systems

TMD was performed on systems F1 to F2 with KWKWK…K sequences. As they are key parts in the opening process the behavior of TM1, TM2 and the cytoplasmic part were monitored by the Cα RMSDs (relative to the starting structure). No constraints were applied to the cytoplasmic domain.

For systems F1, F2 and F3 the Cα RMSD of TM1 showed a significant increase between 1 and 3 ns with a maximum up to 4 Å, then it decreased to 2.5 Å. The variations of TM2 Cα RMSDs were similar for systems F1 to F3. After increasing gradually till 7 ns, it kept stable around 4.5 Å .

The Cα RMSD for F1 and F2 fluctuated around 5 Å during the first 6 ns then reached up to 5.5 Å. For F3 RMDs increased with some fluctuations after 4 ns and reached 8 Å.

The structure of the cytoplasmic domain with protonation of Glu118, Glu120 and His25 (F4 system) went through more significant changes (see below).

Structural comparison with experimental results

Recently, a mutated KcsA system was designed in order to favor the open conformation [34] and a full-length KcsA X-ray structure has been determined [21]. To help crystals generation, Fab2 antibody fragments were employed and, even if X-ray diffraction was obtained at a low resolution (3.9 Å), this permitted a direct and accurate comparison with the closed conformation [21]. However, patch clamp experiments performed for this modified KcsA indicate that this system shows slower kinetics and represents a less open conformation than the natural one [21]. Figure 3 (left) is a superimposition of our final structure with this experimental structure. We performed a structural alignment using the fit module of Multiseq [45] instead of a direct alignment (residue by residue) in order to take into account a possible translation effect of the cytoplasmic domain. As expected, a good fit of the two structures is observed for the channel part of KcsA. The cytoplasmic domain of our model presents a small bending angle which is not observed for the crystal structure. However, the presence of Fab antibodies in the crystallization procedure prevents the

observation of a possible bending angle of the cytoplasmic domain. We also examined a structure from our TMD trajectory that displays a better fit to the experimental full-length KcsA in its open conformation. At 6.3 ns the structural organization of the cytoplasmic domain and the KcsA channel are in very good agreement with the experimental structure (Fig. 3, right). Our simulation procedure thus yields results that are in accordance with experimental results and may show that the experimental X-ray structure of the modified full-length KcsA [21] is an intermediate open state.

The role of pH and the cytoplasmic domain in the opening process

In a recent work, Cuello et al. [4] proposed a shrewd mechanism for proton-dependent gating of the KcsA channel based on a cytoplasmic domain truncated KcsA structure (PDB code 1K4C) together with biochemical experiments. First, they predicted the protonation states of the amino-acids located at the bottom part of the KcsA channel (i.e., the top at the cytoplasmic domain), with electrostatic potential Poisson-Boltzmann computations. Helped by biochemical mutations, they identified four residues that might be involved in the gating process of KcsA: Arg117, Glu120 and Glu118 at the upper part of the cytoplasmic domain and His25 which is located at the start of TM1. According to the low distances between each of these amino-acids, they proposed a seducing mechanism involving electrostatic repulsion to explain the easiest opening of the channel at low pH.

However, the His25 residue is missing on several experimental structures [15, 21, 27, 34] so that its role in the gating process is questionable. Besides, on the experimental full-length KcsA crystal structure the distance between this histidine and the Glu118 residue is around 17 Å. In the truncated structure (PDB code 1K4C) studied by Cuello et al., this distance is about 4.2 Å so that a probable electrostatic interaction was invoked since histidine residues may be protonated at low pH. This ambiguity of the His25 role led us to the design of the two systems F3 and F4, without and with the peptide TM1 tail comprising the His25 residue (see Table 1).

Moreover, several other distances recorded on the truncated KcsA system studied by Cuello et al. are inconsistent with the distances observed on the experimental full-length KcsA structure. For example, the distance between Glu120 and the Arg122 of the facing unit is about 5 Å only in the truncated structure and

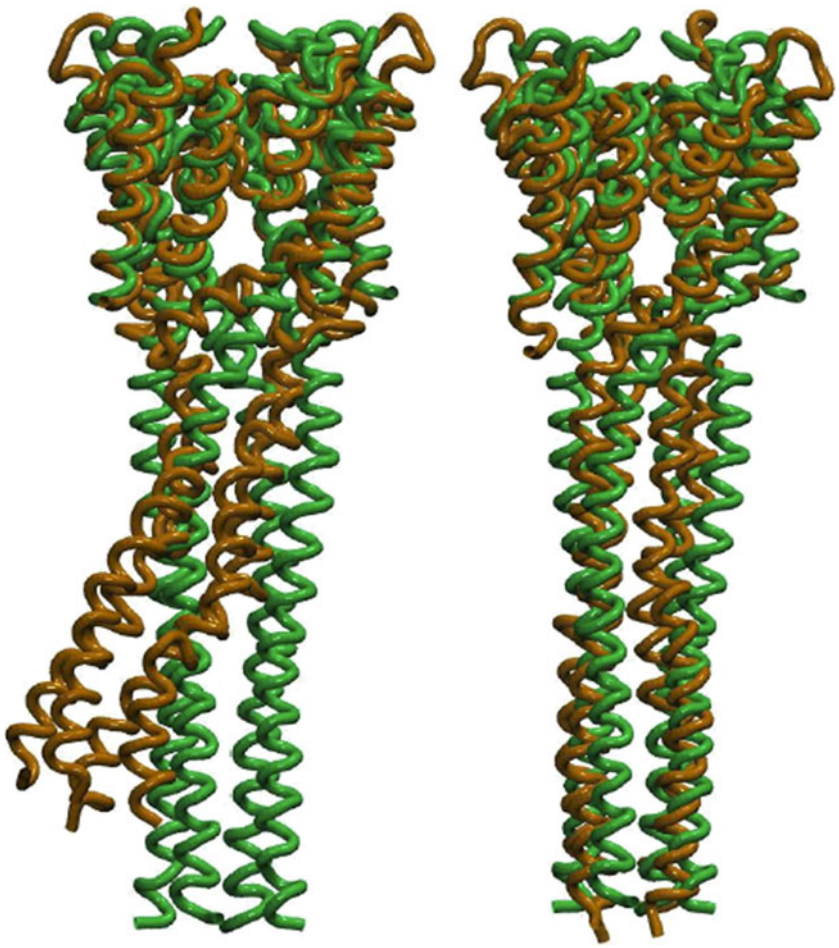

Fig. 3 Comparison of the open full-length KcsA structures obtained in this work (*brown*) and a recent X-ray structure of a constitutively partially open full-length KcsA [21] (*green*). *Left*: superimposition of the final targeted structure generated by the TMD simulation of the F1 system. *Right*: best superimposition with a transient structure of the TMD trajectory around 6.5 ns

around 11.2 Å for the full-length structure. This larger distance drastically abates the proposed strong electrostatic interaction.

However, we performed the conformational transition between closed and opened channel according to the protonation hypothesized by Cuello et al. in order to check whether this mechanism appeared during our TMD simulations.

For the F3 and F4 systems, we did not observe the gating molecular mechanism proposed by Cuello et al. Indeed, the short distances described by this team on a truncated structure were not observed during the TMD trajectory of the full-system, even temporarily or for only one unit. Therefore we feel such interactions cannot be further considered in the gating mechanism. Moreover, the protonation of the eight Glu118 and Glu120 residues, which are negatively charged at neutral pH, unbalances the 16 arginine positive residues (numbers 27, 117, 121 and 122) which are located at the upper part of the cytoplasmic domain. This is shown in Fig. 4 for the F3 system. This cluster of positive charges led to electrostatic repulsions both for systems F3 and F4.

More specifically, for the F4 system, the protonated His25 residues trigger a strong electrostatic repulsion during the first nanosecond that disturbs the TM1 segment helicoid structure (Fig. 5). This movement was unexpected since in all of the open experimental KcsA structures [4, 6, 15, 21, 46], the TM1 fragment retains an α-helix structure. At 3.6 ns the cluster of arginines residues induces a strong electrostatic repulsion that cannot be balanced by the Glu118 and 120 residues which are all neutral. This electrostatic repulsion drastically stretches the α-helix bundle of the cytoplasmic domain. At the end of the TMD simulation (10 ns) the structural organization of the cytoplasmic domain was destroyed. This is inconsistent with the recently published full-length KcsA open structure [21] even if the experimental conditions may have favored a specific organization. Indeed, the presence of Fab2 antibody which helps the crystallization process induces a limited opening of the channel and thus limits the movements of the cytoplasmic domain [21].

The cluster of arginines in the F4 system is present in the F3 system as well. Thus, for this last system, we also observed a strong electrostatic repulsion that cannot be balanced by carboxylate moieties. However, the sequence of events (Fig. 5) during the conformational transition is not completely similar to what we observed for F4. First, from the start up to 7.1 ns, the cluster of arginines residues induces a constant stretch of the cytoplasmic domain alpha helix bundle. This is shown in Fig. 5 at 1.5 ns and 7.1 ns. At this specific time, one strand of the upper part cytoplasmic domain starts a dissymmetric drift and interacts with the TM1 and TM2 fragments of another unit. Two main interactions can explain this behavior: Trp113 of this cytoplasmic strand and Ala109 at the end of TM2 are

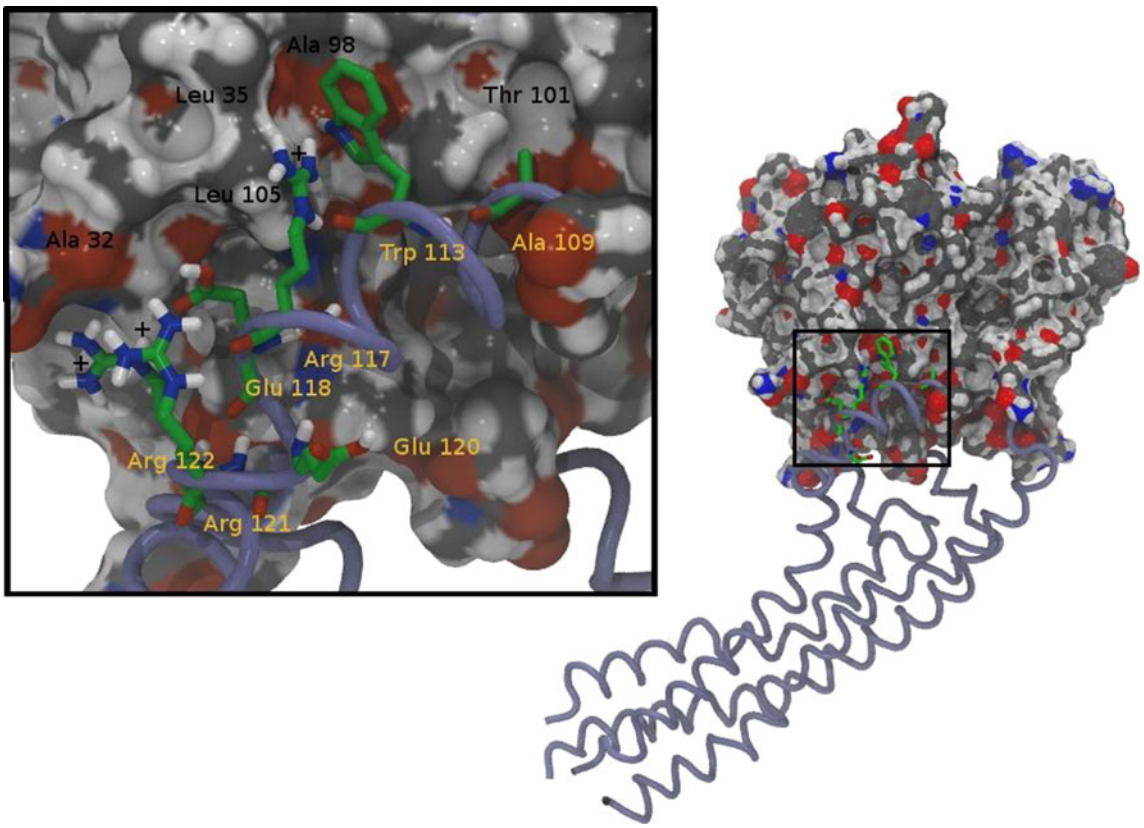

Fig. 4 Structural pattern recorded at 7.1 ns for the F3 system. Molecular surface: transmembrane domain, cyan tubes: cytoplasmic strands

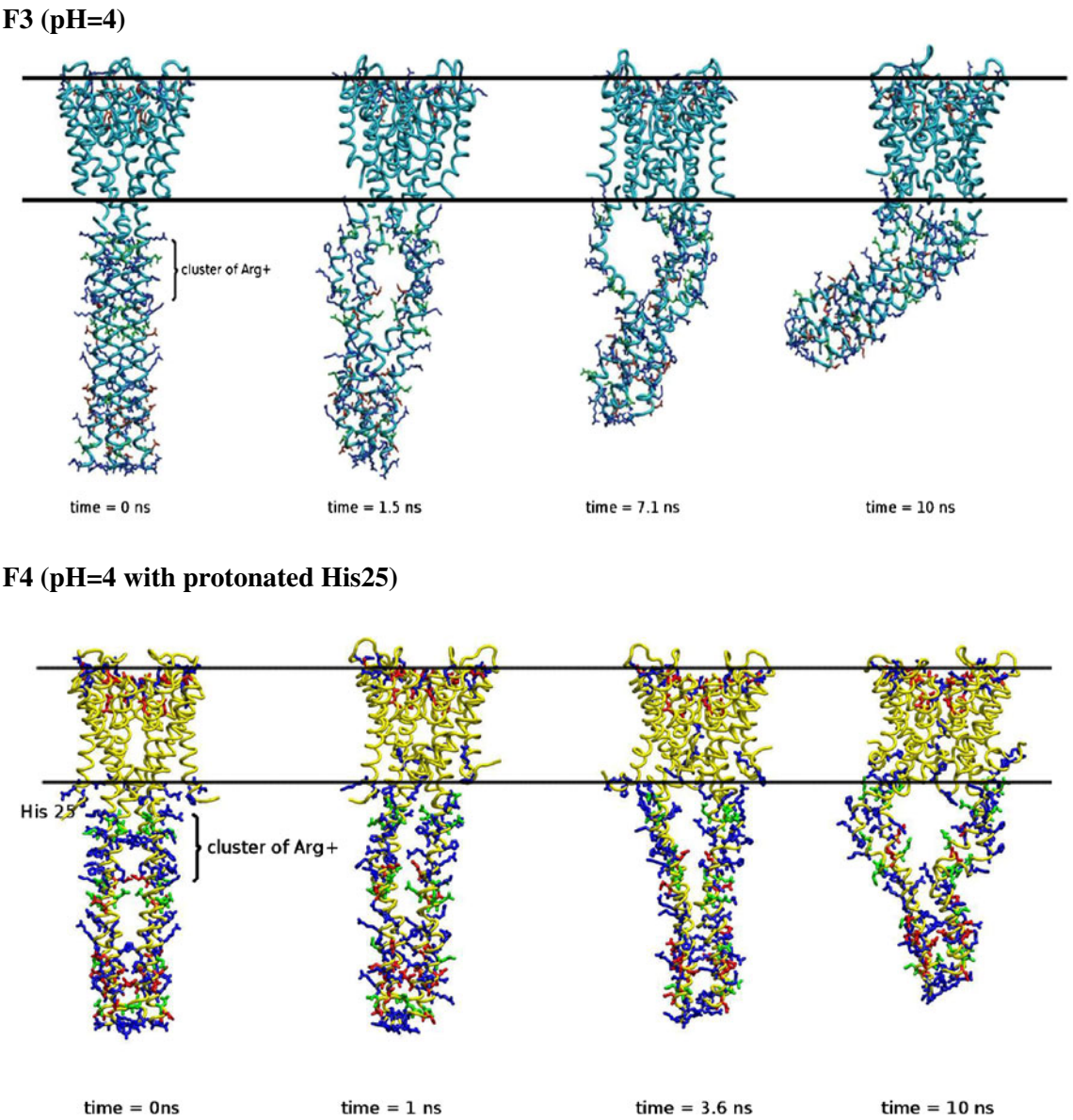

Fig. 5 Snapshots of the TMD opening process for systems F3 and F4 (*top*). *Yellow* (F4) or *cyan* (F3) tubes: overall backbone structure of the full length KcsA *blue and red*: positively and negatively charged residues, respectively *green*: Protonated aspartic and glutamic acids (neutral) location of His25 and the cluster of Arginines 27, 117, 121 are shown. The two horizontal lines provide a schematic view of the membrane

inserted in a hydrophobic cavity, composed by residues Leu35 (TM1), Ala98, Thr101 and Leu105 (TM2), whereas the Arg117 residue has a stabilizing electrostatic interaction with the carbonyl moiety of the Ala32 (TM1). Figure 4 illustrates these interactions. After the conformational transition induced by the TMD simulations, the overall structure of the F3 system presents a large bending angle of its cytoplasmic domain (65°—see Fig. S1 in Supplementary data). This structural feature means that a part of the cytoplasmic domain penetrates and remains in the membrane during the gating process. This is inconsistent with all experimental observations.

The C-terminal pH sensor domain

As stated above, to determine the protonation states of the cytoplasmic domain at pH 4 and 7, we used the H++ calculation [37]. It can be pointed out that, either at pH=7 or pH=4, the eight Glu118 and Glu122 residues show a similar protonation scheme, i.e., only one Glu118 residue out of four is protonated (Table 1). This fact also emphasizes previous results demonstrating that the pH probe sensor is not located on the upper part of the cytoplasmic domain. At low pH (pH=4, system F1) the 12 histidine residues (His124, His128 and His145) are all protonated and thus positively charged whereas these remain

Table 3 Binding energy values (kcal mol^{-1}) determined with the MMGBSA method for the full-length KcsA F1 and F2 systems (top) and the cytoplasmic domain only (bottom)

Full-length KcsA	F1 (pH=4)	F2 (pH=7)
Gas phase		
ΔE_{elec}	4464.9±0.8	−706.8±1.6
ΔE_{vdw}	−755.7±3.0	−786.8±2.3
ΔE_{gas}	3709.2±3.8	−1493.6±3.9
Solvent phase		
$\Delta G_{non\text{-}polar}$	−124.3±0.1	−123.5±0.1
ΔG_{GB}	−4400.0±1.7	730.7±1.5
$\Delta G_{solvant}$	−4524.4±1.8	607.2±1.6
Total		
$\Delta G_{elec} = \Delta G_{GB}+\Delta E_{elec}$	64.9±2.6	23.9±3.2
$\Delta G=\Delta E_{gas}+\Delta G_{non\text{-}polar}+\Delta G_{solvent}$	−815.2±5.7	−886.3±5.5
Cytoplasmic domain	F1 (pH=4)	F2 (pH=7)
Gas phase		
ΔE_{elec}	3988.8±1.5	−825.3±3.4
ΔE_{vdw}	−406.2±1.6	−428.8±1.1
ΔE_{gas}	3582.7±3.1	−1254.1±4.5
Solvent phase		
$\Delta G_{non\text{-}polar}$	−70.8±0.1	−70.22±0.3
ΔG_{GB}	−4019.0±2.2	752.8±2.9
$\Delta G_{solvant}$	−4089.8±2.3	682.5±3.2
ΔG_{elec}	−30.2±3.7	−72.6±7.3
$\Delta G=\Delta E_{gas}+\Delta G_{non\text{-}polar}+\Delta G_{solvent}$	−507.1±2.9	−571.6±7.7
Solute entropy $T\Delta S_{gas}$	186.2±2.4	174.0±2.2
ΔG_{total}	−693.3±5.3	−745.6±9.9

neutral at pH=7 (system F2). For the acidic residues (Asp and Glu) the prediction of the protonation is more complex: even at low pH, some residues still bear a negative charge and some are neutral at pH 7. Table 1 shows the various protonations of the cytoplasmic domain of F1 and F2.

We visualized the opening process induced by the TMD simulation and focused our analyses on the cytoplasmic domain which was free to move during these simulations. For both systems, F1 and F2, the bundle folding of the four cytoplasmic alpha-helix remained organized during the opening process. As a consequence, only small bending[2] angles were recorded for the F1 (26°) and F2 systems (9°). This fact is in accordance with several experimental observations [6, 13, 21] and thus partly validates our simulations. Since only small structural modifications of cytoplasmic domain global structure occurred during the opening process, we calculated free energies of binding with the MMGBSA method.

Entropy calculations were performed for the cytoplasmic domain only since the TM part was restrained. This calculation was not performed for systems F3 and F4 because of the large structural changes of this domain during the corresponding simulations.

Table 3 allows a first comparison of the ΔG values (=$\Delta E_{gas}+\Delta G_{non\text{-}polar}+\Delta G_{solvent}$, not including solute entropies) for the full-length KcsA and the cytoplasmic domain. This indicates that the F2 system is more stable by *ca*. −70 kcal mol^{-1} and this value is similar for the full-length KcsA or the cytoplasmic domain alone. Of course the energy difference that we observed between F1 and F2 is due to the cytoplasmic domain only since we studied the role of protonation in this domain only.

Another major difference appeared for the gas phase electrostatic components of the two systems. Indeed, positive values at low pH (+4464.9 and +3988.8 kcal mol^{-1} for the full-length KcsA and the cytoplasmic domain alone, respectively) were observed, whereas these are negative at neutral pH (−706.8 and −825.3 kcal mol^{-1} for the whole KcsA and the cytoplasmic domain only). For F1, the positive values were counterbalanced by a low value of the solvent electrostatic contribution, but they have no real meaning for the full-length KcsA because part of the real system is inserted in a membrane.

Therefore, in the conditions used for our simulations, only an analysis of the cytoplasmic domain may have significance and thus we added the solvent to the gas phase electrostatic components to obtain electrostatic free energies (ΔG_{elec}, Table 3). With values of −30.2 kcal/mol^{-1} for the F1 system and −72.6 kcal mol^{-1} for the F2 system, it appears again that the difference in global binding energy of the KcsA channel is also depending on the electrostatic contribution of the cytoplasmic domain. This suggests that specific amino-acids protonation triggers, or at least helps, the opening process of this channel.

Finally when solute entropy contributions are added, it is clear that the change of pH from 4 to 7 induces a stabilization of the cytoplasmic domain of *ca*. 52 kcal mol^{-1}.

These results show that it is easier to open the channel at low pH than at neutral pH and confirm that the cytoplasmic domain indeed plays a role in the pH dependent behavior of the system. They are in this respect globally in agreement with the experimental results of Hirano et al. [33].

We further analyzed and compared the TMD trajectories of both systems and focused our attention on the cytoplasmic residues which have different protonation patterns at the two pH values. We finally propose a sequence of events that could account for part of the opening process of the KcsA channel.

Role of His124, 128 and 145

The Histidines 124 of the four units are orientated toward the solvent and thus are all protonated at low pH (Fig. 6). During the first 0.5 ns of the trajectory, these positively charged histidines interact strongly and durably

[2] The global bending of the cytoplasmic domain was defined by the angle between the mass-weighted backbone atoms of residues Val48, Ala111 and Asp120 of the four units.

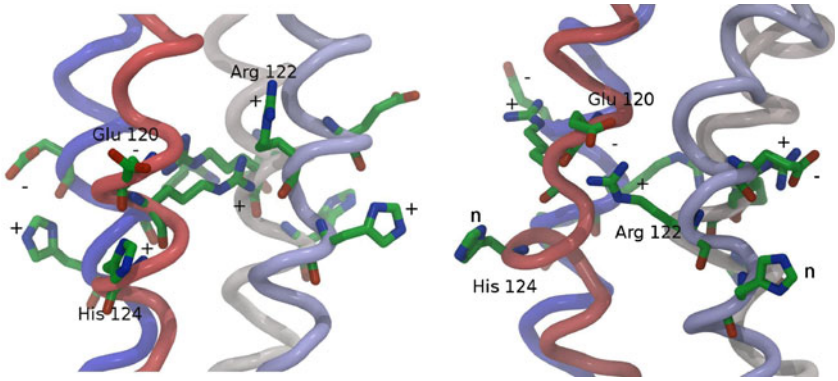

Fig. 6 The specific role of His124 at low pH (*left*) or at neutral pH (*right*). See text for details. The charges of residues are shown

with the negatively charged Glu120 of its own unit. At neutral pH, the histidines 124 are not bearing a positive charge and do not counterbalance Glu120. This last residue shows a strong interaction, again around 0.5 ns and durably, with the arginine 122 of the vicinal unit (Fig. 6). These specific electrostatic interactions steadily associate the cytoplasmic strands and hamper the opening process at pH=7. At low pH the protonation of His124 suppresses these interactions. This result may explain Cuello's hypothesis [4] (F3 and F4 systems) as well as the results of Thompson [17] who emphasized the role of a neutral Glu120 to help the gating of KcsA. Our results suggest here that the Glu120 residues are not protonated but engaged, at low pH, in an intra-strand salt-bridge which weakens the cytoplasmic interaction and then favors channel opening.

Histidines 128 are, in sequence, located at a distance of four residues to His124. Therefore, according to the α-helix organisation, these are also highly exposed to the solvent and this explains their protonation at low pH. After careful observation, it appears that the His128 residues are not engaged in specific interactions either at low or neutral pH. As a consequence, we expect only small electrostatic repulsions at pH=4 where these residues bear positive charges. To better observe this, and since these amino-acids roughly define a square, we recorded the perimeter of their side chains as a function of time (Fig. 7). It may be pointed out that, at low pH, the variation of these distances is more important than at neutral pH for which the distance is constant. Moreover, with a perimeter average value of 68.1 Å at pH=4 instead of 62.3 Å at pH=7, this evidences weak electrostatic repulsions of the His128 residues that help the opening of the channel at low pH.

We found a similar role for Histidines 145 with an average perimeter values of 56.7 Å at pH=4 and 52.1 Å at pH=7.

Role of Glu130, Glu134 and Glu135

At acidic pH, two of the four Glu130 residues are protonated and are thus neutral whereas at pH 7, all the Glu 130 amino-acids bear a negative charge. We examined the role of these residues during the gating induced by the TMD. At pH 7 we observed, all along the trajectory, intra-strand electrostatic interactions between the negative charges of Glu130 and the positive charges of Arg127. When the pH is low, after 2 ns, the two protonated Glu130 no longer interact with the positive charges of Arg127 so that these residues induce inter-strand repulsion (Fig. 8). These electrostatic repulsions help the opening of the KcsA channel.

All Glu134 residues are neutral at low pH whereas only two of them are protonated at neutral pH. For the Glu135 residues, all bear one negative charge whereas two of them, of units B and D, are protonated and thus neutral. When they are negatively charged the Glu134

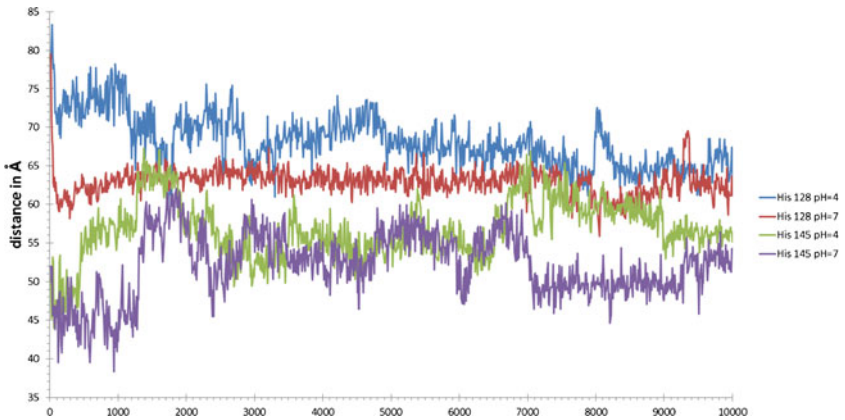

Fig. 7 Side chains perimeters of the His128 and His145 residues at pH=4 and pH=7

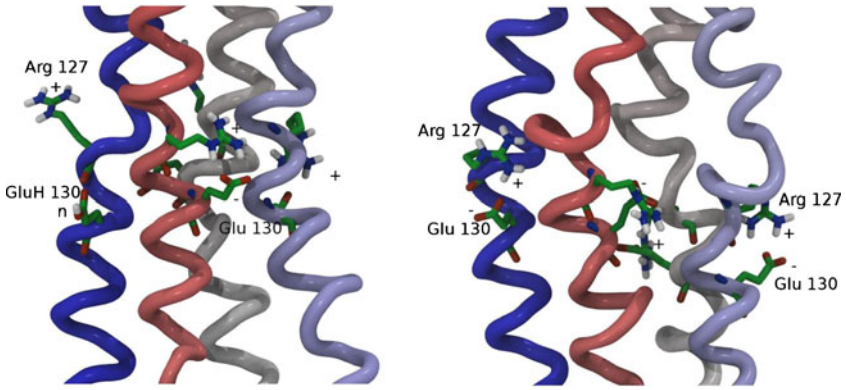

Fig. 8 The role of Glu130 residues at pH 4 (*left*) and pH 7 (*right*). Picture taken at 2 ns of the targeted molecular dynamics trajectories. See text for details. The charges of amino-acids are shown (n = neutral)

residues are shielding the Lys131 ammonium cations of their own strand. At acidic pH, these interactions are missing or weak and thus Lys131 induces electrostatic repulsions that favor the opening process. We found a similar behavior, at neutral pH, for the Glu135 amino-acids which interact with the Arg139 positive charges of their own strand. Again, this shielding decreases the electrostatic repulsion of the cytoplasmic domain that helps the gating of KcsA. Furthermore, a specific inter-unit interaction occurs around 5 ns of the trajectory. One Glu135 makes a strong, but transient (for around 1 ns), interaction with the Arg139 of the vicinal strand. We also observed the symmetric behavior but this interaction appears weaker and is not present during all of the trajectory duration. When protonated, the Glu135 residues are not able to produce these inter-strand interactions that tend to maintain the KcsA channel in the closed state. Figure 9 summarizes these interactions.

Role of Asp156 and 157

Several ionizable residues are located at the end of the cytoplasmic domain sequence of KcsA. The four aspartic acids 156 are all neutral at low pH whereas only two of them are neutral at pH 7 (Table 1). Besides, all aspartic acids at position 157 are negatively charged at pH=7 but one of them is protonated at pH=4. During the opening of the channel induced by the TMD, this part of the structure is the more twisted probably because the end of the cytoplasmic domain is more flexible. At neutral pH, these aspartate anions are shielded by the vicinal arginines 153 and 159 which are all cationic. Moreover, the C-terminal residues 159 are negative. Therefore, at pH=7, all these ions interfere together and produce stable interactions. Precisely, after 7 ns a durable interaction occurs which is illustrated in Fig. 10: the Arg159 residue, of one unit, intervenes through electrostatic interactions with the Asp157 of its own unit and the C-terminal part of a neighboring unit. At acidic pH, through the neutralization of the aspartic acids mentioned above, these stable interactions disappear or are weaker and hence promote the conformational transition observed during the KcsA gating.

Role of Glu146 and Asp149

As mentioned above, Hirano et al. [33] found that when both residues Glu146 and Asp149 are mutated to Gln 146 and Asn 149 the KcsA channel is no longer pH dependent and opens easily. We thus examined the role of these residues in our simulations.

Two of the four Glu146 residues, belonging to opposite units, are predicted to be protonated at acidic pH and thus, become neutral by losing their negative

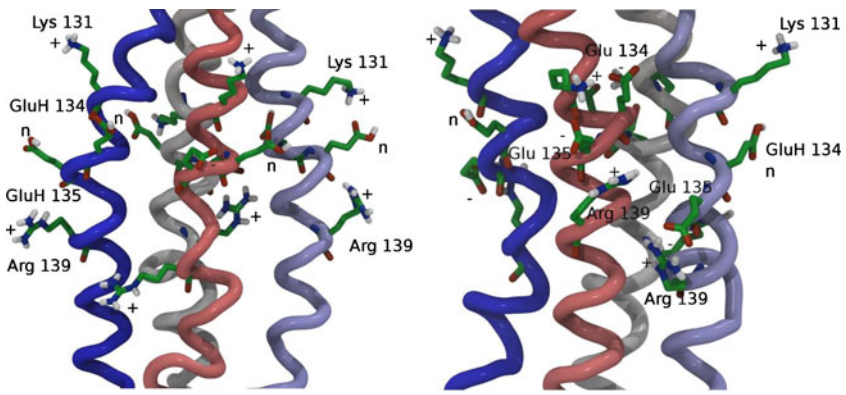

Fig. 9 The role of Glu134 and 135 residues at pH 4 (*left*) and pH 7 (*right*). Picture taken at 5 ns of the TMD trajectories. See text for details. The charges of amino-acids are shown (n = neutral)

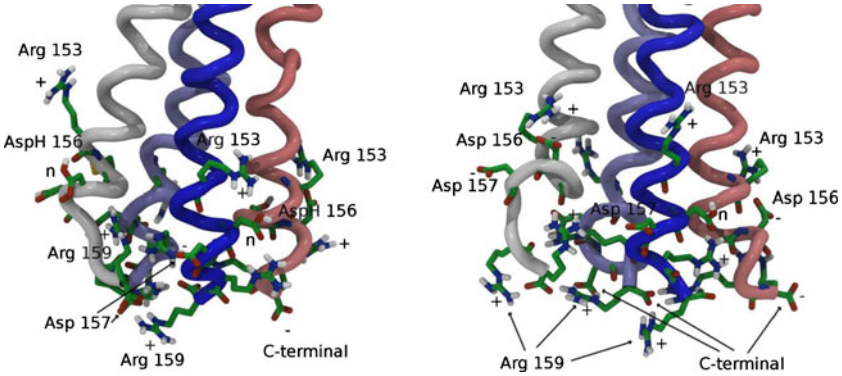

Fig. 10 The role of Asp156 and 157 residues at pH 4 (*left*) and pH 7 (*right*). This picture is taken at 7 ns of the TMD trajectories. See text for details. The charges of amino-acids are shown (n = neutral)

charge. At physiological pH, we observe that the glutamates 146 are involved in strong electrostatic interactions with Arg142 of the same strand. These interactions, roughly observed all along the trajectory, shield the positive charge of Arg142 residues. At low pH, the protonation of the two Glu146 residues results in the suppression of these interactions: the Arg142 amino-acids then act as repulsive inter-strand forces. This favors the opening process of KcsA. This confirms and explains the role of Glu146. Figure 11 summarizes these facts.

However, we did not predict a protonation change for Asp149 which stays as aspartate, and thus bears negative charges at both pH values (Table 1). The role of Asp149 in our TMD trajectories was thus similar at acidic or neutral pHs. We observed that, from *ca*. 2 ns to the end of the opening process, the Asp149 residue of one strand was involved in a salt bridge with the Arg147 residue of the neighboring strand (see Fig. S2 in Supplementary data). These four strong electrostatic interactions stabilize the bundle of α helices and help maintain the structural integrity of the cytoplasmic domain. It thus seems that when coupled with the mutation of Glu146 [33] the neutralization of Asp149 into asparagine destroys this anchoring between the α helices and facilitates the opening process.

Conclusions

Recent literature clearly indicates that the cytoplasmic domain plays a role in pH sensing, for instance the above-mentioned recent work by Hirano et al. [33]. The important results of Cuello et al. working with a truncated system [4] represented the first detailed analysis of a molecular gating mechanism based on electrostatic interactions of some residues.

Using TMD we have performed, for the first time, a simulation of the opening of full-length KcsA, focusing our interest on the cytoplasmic domain. We used several systems devised from literature results at pH 4 and pH 7. Satisfactory structural comparisons with recent experimental results validate our simulation procedure.

Free energy calculations and a comparison of our full-length systems at pH 4 and pH 7 clearly show a stabilization at pH 7, showing that specific amino-acids protonation in the cytoplasmic domain play a role in the opening process.

Finally, a careful analysis of the protonated residues and their interactions has permitted to find the precise role of some of them such as His124, 128 and 145, Glu130, 134 and 135, Asp156 and 157 as well as Glu146 and Asp149 already experimentally shown to be important residues in

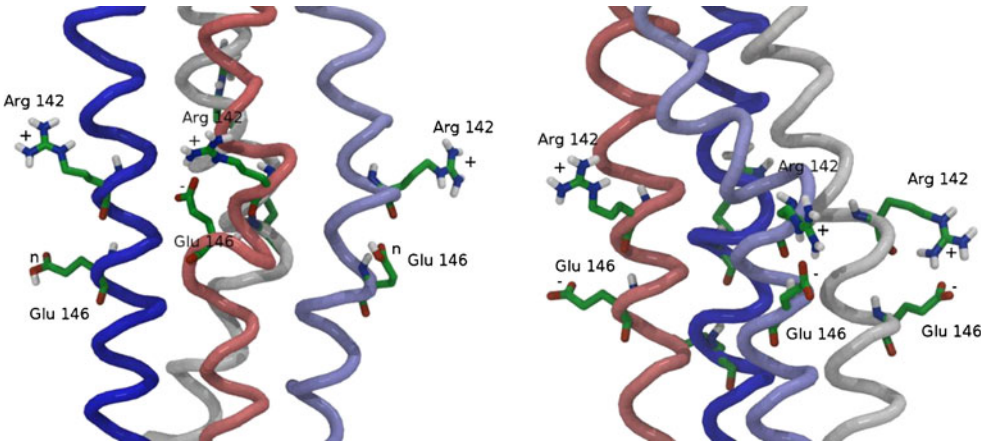

Fig. 11 The role of Glu146 residues at pH 4 (*left*) and pH 7 (*right*). Picture taken at 2 ns of the TMD trajectory. See text for details. The charges of amino-acids are shown (n = neutral)

the process [33]. The role of His 25 invoked by several authors remains unclear.

Another possibly interesting feature from our results is that the ionizable residues located near the transmembrane domain act quickly, within the first nanosecond, so that they certainly help trigger the opening process. As the cytoplasmic sequence proceeds, the above-described events appear later in the TMD trajectory so that these structural changes are gradually transmitted to help the KcsA gating. This confirms that pH sensing is due to both domains: the cluster region on the boundary of internal membrane, together with the cytoplasmic part.

Acknowledgments The China Scholarship Council is gratefully acknowledged for granting a PhD scholarship to Yan LI.

References

1. Hille B (2003) Ion channels of excitable membranes, 3rd edn. Sinauer, Sunderland, MA
2. Alagem N, Yesylevskyy S, Reuveny E (2003) The pore helix is involved in stabilizing the open state of inwardly rectifying K+ channels. Biophys J 85:300–312
3. Krol E, Trebacz K (2000) Ways of ion channel gating in plant cells. Ann Bot 86:449–469
4. Cuello LG, Cortes DM, Jogini V, Sompornpisut A, Perozo E (2010) A molecular mechanism for proton-dependent gating in KCSA. FEBS Lett 584:1126–1132
5. Salkoff L, Wei AD, Baban B, Butler A, Fawcett G, Ferreira G, Santi CM (2005) The *C. elegans* research community, WormBook, doi:10.1895/wormbook.1.42.1
6. Uysal S, Vasquez V, Terechko V, Esaki K, Koide S, Fellouse FA, Sidhu SS, Perozo E, Kossiakoff A (2009) The crystal structure of full-length KcsA in its closed conformation. Proc Natl Acad Sci USA 106:6644–6649
7. Cuello LG, Romero JG, Cortes DM, Perozo E (1998) pH-dependent gating in the Streptomyces lividans K channel. Biochemistry 37:3229–3236
8. Heginbotham L, LeMasurier M, Kolmakova-Partensky L, Miller C (1999) Single streptomyces lividans K+channels: functional asymmetries and sidedness of proton activation. J Gen Physiol 114:551–560
9. Schrempf H, Schmidt O, Kümmerlen R, Hinnah S, Müller D, Betzler M, Steinkamp T, Wagner R (1995) A prokaryotic potassium ion channel with two predicted transmembrane segments from Streptomyces lividans. EMBO J 14:5170–5178
10. Doyle DA, Morais Cabral J, Pfuetzner RA, Kuo A, Gulbis JM, Cohen SL, Chait BT, MacKinnon R (1998) The structure of the potassium channel: molecular basis of K+conduction and selectivity. Science 280:69–77
11. Zhou Y, Morais-Cabral JH, Kaufman A, MacKinnon R (2001) Chemistry of ion coordination and hydration revealed by a K^+ channel-Fab complex at 2.0 Å resolution. Nature 414:43–48
12. Pau VP, Zhu Y, Yuchi Z, Hoang QQ, Yang DS (2007) Characterization of the C-terminal domain of a potassium channel from Streptomyces lividans (KcsA). J Biol Chem 282:29163–29169
13. Cortes DM, Cuello LG, Perozo E (2001) Molecular architecture of full-length KcsA: role of cytoplasmic domains in ion permeation and activation gating. J Gen Physiol 117:165–180
14. Perozo E, Cortes DM, Cuello LG (1999) Structural rearrangements underlying K1-channel activation gating. Science 285:73–78
15. Liu YS, Sompornpisut P, Perozo E (2001) Structure of the KcsA channel intracellular gate in the open state. Nat Struct Biol 8:883–887
16. Jiang Y, Lee A, Chen J, Ruta V, Cadene M, Chait BT, MacKinnon R (2002) The open pore conformation of potassium channels. Nature 417:523–526
17. Thompson AN, Posson DJ, Parsa PV, Nimigean CM (2008) Molecular mechanism of pH sensing in KcsA potassium channels. Proc Natl Acad Sci USA 105:6900–6905
18. Takeuchi K, Takahashi H, Kawano S, Shimada I (2007) Identification and characterization of the slowly exchanging pH-dependent conformational rearrangement in KcsA. J Biol Chem 282:15179–15186
19. Shen Y, Kong Y, Ma J (2002) Intrinsic flexibility and gating mechanism of the potassium channel KcsA. Proc Natl Acad Sci USA 99:1949–1953
20. Hirano M, Takeuchi Y, Aoki T, Yanagida T, Ide T (2010) Rearrangements in the KcsA cytoplasmic domain underlie its gating. J Biol Chem 285:3777–3783
21. Uysal S, Cuello LG, Cortes DM, Koide S, Kossiakoff AA, Perozo E (2011) Mechanism of activation gating in the full-length KcsA K+channel. Proc Natl Acad Sci USA 108:11896–11899
22. Zhong W, Guo W (2009) Mixed modes in opening of KcsA potassium channel from a targeted molecular dynamics simulation. Biochem Biophys Res Comm 388:86–90
23. Compoint M, Picaud F, Ramseyer C, Girardet C (2005) Zip gating of the KcsA channel studied by targeted molecular dynamics. Chem Phys Lett 407:199–204
24. Compoint M, Picaud F, Ramseyer C, Girardet C (2005) Targeted molecular dynamics of an open-state KcsA channel. J Chem Phys 122:134707–134714
25. Zhong W, Guo W, Ma S (2008) Intrinsic aqueduct orifices facilitate K+channel gating. FEBS Lett 582:3320–3324
26. Holyoake J, Domene C, Bright JN, Sansom MS (2004) KcsA closed and open: modelling and simulation studies. Eur Biophys J 33:238–246
27. Cuello LG, Jogini V, Cortes DM, Perozo E (2010) Structural mechanism of C-type inactivation in K^+ channels. Nature 466:203–208
28. Compoint M, Carloni P, Ramseyer C, Girardet C (2004) Molecular dynamics study of the KcsA channel at 2.0 Å resolution: Stability and concerted motions within the pore. Biochim Biophys.Acta, 1661:26–39
29. Morais-Cabral JH, Zhou Y, MacKinnon R (2001) Energetic optimization of ion conduction rate by the K+selectivity filter. Nature 414:37–42
30. Raja M (2010) The role of extramembranous cytoplasmic termini in assembly and stability of the tetrameric K(+)-channel KcsA. J Membrane Biol 235:51–61
31. Heginbotham L, Odessey E, Miller C (1997) Tetrameric stoichiometry of a prokaryotic K+channel. Biochemistry 36:10335–10342
32. Meuser D, Splitt H, Wagner R, Schrempf H (1999) Exploring the open pore of the potassium channel from *Streptomyces lividans*. FEBS Lett 462:447–452
33. Hirano M, Onishi Y, Yanagida T, Ide T (2011) Role of the KcsA channel cytoplasmic domain in pH-dependent gating. Biophys J 101:2157–2162
34. Cuello LG, Jogini V, Cortes DM, Sompornpisut A, Purdy MD, Wiener MC, Perozo E (2010) Design and characterization of a constitutively open KcsA. FEBS Lett 584:1133–1138

35. Cuello LG, Jogini V, Cortes DM, Pan AC, Gagnon DG, Dalmas O, Cordero-Morales JF, Chakrapani S, Roux B, Perozo E (2010) Structural basis for the coupling between activation and inactivation gates in K(+) channels. Nature 466:272–275
36. Kharkyanen VN, Yesylevskyy SO, Berezetskaya NM, Boiteux C, Ramseyer C (2009) Semi-quantitative model of the gating of KcsA ion channel. 2. Dynamic self-organization model of the gating Biopolym. Cell 25:476–483
37. Andersen HC (1980) Molecular dynamics at constant pressure and/or temperature. J Chem Phys 72:2384–2393
38. Gordon JC, Myers JB, Folta T, Shoja V, Heath LS, Onufriev A (2005) H++: a server for estimating pKas and adding missing hydrogens to macromolecules. Nucleic Acids Res 33:W368–W371
39. Schlitter I, Engels M, Krüger P (1994) Targeted molecular dynamics: a new approach for searching pathways of conformational transition. J Mol Graphics 12:84–89
40. Karplus M, Kuriyan J (2005) Molecular dynamics and protein function. Proc Natl Acad Sci USA 102:6679–6685
41. Case D, Darden T, Cheatham TE, Simmerling C, Wang J, Duke, Luo R, Crowley M, Walker R, Zhang W, Merz K, Wang B, Hayik S, Roitberg A, Seabra G, Kolossvary I, Wong K, Paesani F, Vanicek J, Wu X, Brozell S, Steinbrecher T, Gohlke H, Yang L, Tan C, Mongan J, Hornak V, Gui G, Mathews D, Seetin M, Sagui C, Babin V, Kollman P (2010) AMBER 11, University of California, San Francisco
42. Ryckaert JP, Ciccotti G, Berendsen HJC (1977) Numerical integration of the cartesian equations of motion of a system with constraints: molecular dynamics of N-alkanes. J Comput Phys 23:327–341
43. Kottalam J, Case D (1990) Langevin modes of macromolecules: applications to crambin and DNA hexamers. Biopolymers 29:1409–1421
44. Jörg W, Peter SS, Still WC (1999) Approximate atomic surfaces from linear combinations of pairwise overlaps (LCPO). J Comput Chem 20:217–230
45. Roberts E, Eargle J, Wright D, Luthey-Schulten Z (2006) Multiseq: unifying sequence and structure data for evolutionary analysis. BMC Bioinforma 7:382–393
46. Chen X, Poon BK, Dousis A, Wang Q, Ma J (2007) Normal-mode refinement of anisotropic thermal parameters for potassium channel KcsA at 3.2 Å crystallographic resolution. Structure 15:955–962